Phil. Trans. R. Soc. B
Volume 362, Number 1487 / November 29, 2007
http://dx.doi.org/10.1098/rstb.2007.2079

Motility and autotoxicity in *Karenia mikimotoi* (Dinophyceae)

P. Gentien[1,*], M. Lunven[1], P. Lazure[1], A. Youenou[1], M.P. Crassous[1]

[1]IFREMER, DYNECO, Centre de Brest, B.P.70, 29280 Plouzané, France

*: Corresponding author : Patrick.Gentien@ifremer.fr

Abstract:

Karenia mikimotoi is one of the most common red-tide dinoflagellates proliferating in the eastern North Atlantic and around Japan. Kills of marine fauna are associated with its blooms. In mixed water columns it migrates vertically, while in stratified water columns, the population remains confined within pycnocline layers. Wind events, increasing mixing and agitation initiate declines in its populations. This paper is focused on the formulation of mortality rate relative to shear rate. Autotoxicity is demonstrated by the use of a synthetic toxin. Bioconvection observed in cultures allows the establishment of a trade-off between phototropism, which leads to the local accumulation of cells, and their autotoxicity, which would prevent cell concentration. The combination of these processes allows diffusion of the toxin into the underlying water, where it subsequently degrades. Confinement of the population in the pycnocline layer results also from another trade-off between growth conditions and shear-rate-modulated mortality. A simplified encounter kernel was introduced into the population dynamics equation to account for a mortality factor. Under realistic forcing conditions with a small number of parameters, this model reproduced the confinement of the population in the pycnocline layer, the proper timing and the duration of the recurrent *K. mikimotoi* bloom on the Ushant front (France).

PHILOSOPHICAL TRANSACTIONS OF THE ROYAL SOCIETY B

Phil. Trans. R. Soc. B
doi:10.1098/rstb.2007.2079

Motility and autotoxicity in *Karenia mikimotoi* (Dinophyceae)

P. Gentien*, M. Lunven, P. Lazure, A. Youenou and M. P. Crassous

IFREMER, DYNECO, Centre de Brest, B.P.70, 29280 Plouzané, France

Karenia mikimotoi is one of the most common red tide dinoflagellates proliferating in the eastern North Atlantic and around Japan. Kill of marine fauna is associated with its blooms. In mixed water columns, it migrates vertically while in stratified water columns, the population remains confined within pycnocline layers. Wind events, increasing mixing and agitation, initiate declines in its populations. This paper is focused on the formulation of mortality rate relative to shear rate. Autotoxicity is demonstrated by the use of the synthetic toxin. Bioconvection observed in cultures allow the establishment of a trade-off between phototropism that leads to the local accumulation of cells and their autotoxicity which would prevent cell concentration. The combination of these processes allows diffusion of the toxin into the underlying water, where it subsequently degrades. Confinement of the population in the pycnocline layer results also from another trade-off between growth conditions and shear-rate-modulated mortality. A simplified encounter kernel was introduced into the population dynamics equation to account for a mortality factor. Under realistic forcing conditions with a small number of parameters, this model reproduced the confinement of the population in the pycnocline layer, the proper timing and the duration of the recurrent *K. mikimotoi* bloom on the Ushant front (France).

Keywords: autotoxicity; allelopathy; ichthyotoxicity; bioconvection; encounter rate

1. INTRODUCTION

Known in the literature successively under different names (*Gyrodinium aureolum*, *Gymnodinium* cf. *aureolum*, *G. nagasakiense*, *G. mikimotoi*), *Karenia mikimotoi* is one of the most common red tide dinoflagellate proliferating in the eastern North Atlantic regions and around Japan. Blooms of this species are commonly associated with kill of marine fauna. The vegetative niche of this species has been outlined by Gentien (1998).

In the case of mixed or slightly stratified water columns, *K. mikimotoi* is observed to vertically migrate daily with a range of up to 15 m (Koizumi *et al*. 1996). When stratification is greater, the population exhibits a non-migrating maximum in the pycnocline layer (Bjoernsen & Nielsen 1991; Arzul *et al*. 1993), relying mainly on nitrogen remineralization (Le Corre *et al*. 1993). It is not possible to estimate from the available data the lowest density gradient through which migration still persists. The reasons of this shift in behaviour have not yet been elucidated, but they are of great importance when modelling is done in view of prediction.

Sharp pycnocline layers are associated with high shear between water mass and, if phototropism modulated by cell quota were the only driving force behind population movement, cells escaping from the transition zone would flush out: observations of high concentrations forming layers could be partly the result of this selection. Even if fine layering can result from purely physical processes (Franks 1995), persistence of populations in narrow layers at small scale suggests that other factors, such as chemotropism or higher survival rates in layers of low turbulent energy, may be involved in the maintenance of high-concentration populations within these layers. Maintenance and growth of the population is possible, considering the temperature and light regimes at these depths. These boundary layers may also exhibit limited residual movement, allowing the population to develop with limited dispersion. In this paper, we address the possibility of higher survival rates in pycnocline layers.

Increased stability of the water column due to stratification and calm weather is generally favourable to red tides, while storm events terminate them (see Iizuka *et al*. 1989). Wind strength tends to be inversely related to bloom maintenance (Yamamoto & Seike 2003). Physical–biological interactions at small scale may have different effects on dinoflagellates, including lowering the growth rate (Pollingher & Zemel 1981; Juhl & Latz 2002; Sullivan *et al*. 2003) associated sometimes with increased mortality and changes in morphology (Berdalet 1992). However, the threshold for the appearance of such negative effects is species specific (Sullivan *et al*. 2003). Although the above-cited works involved thecate dinoflagellates, similar effects may also apply to *K. mikimotoi*, which is athecate. Even if commonly observed and reported, the major processes underlying these effects have never been formulated in population models.

In the case of *K. mikimotoi*, the effect does not seem to be a repression in growth rate due to the arrest of

*Author for correspondence (pgentien@ifremer.fr).

One contribution of 18 to a Theme Issue 'Environmental constraints upon locomotion and predator–prey interactions in aquatic organisms'.

the cell cycle. Agitation in cultures reduces the cell concentration to the point that specific care in manipulating cultures has to be taken. This species produces exotoxins with a haemolytic effect due to the non-specific inhibition by 18 : 5n3 fatty acid of membrane ATPases (Fossat *et al.* 1999). By preventing osmoregulation, it could be that the same toxin kills *K. mikimotoi* while inhibiting competitors (Gentien & Arzul 1990), killing fishes and other organisms (Sola *et al.* 1999) and deforming bivalve shells (Erard-Le Denn *et al.* 1990). We report here the role of this toxin in the sensitivity of *K. mikimotoi* to agitation.

Here, we report the autotoxicity demonstrated using the synthetic toxin. From detailed studies conducted in still cultures, we examine the trade-off between cell concentration induced by phototropism and autotoxicity. A simplified formulation of the collision kernel was applied to a one-dimensional model with realistic forcing in order to test the importance of this control process on population dynamics.

2. MATERIAL AND METHODS

(a) *Cell cultures and sampling*

Karenia mikimotoi cells were sampled during a toxic bloom from the Rade de Brest, France. The cells isolated were batch cultured without agitation in a sterile Guillard's f/2 medium at 18 ± 1°C under a 12 h : 12 h light : dark cycle at 60 μE m^2 s^{-1}. Since the species is very sensitive to agitation, special care was taken in homogenizing the cultures, prior to sampling: the same person always did the mixing, very gently, before sampling, thus ensuring the best reproducibility. Repartition into aliquots was done at least 12 h prior to experimentation in order to limit the numbers of non-viable cells. Samples were taken either by syringe or by siphoning into tubes previously filled with the required amount of Lugol's fixative. Maximum growth rate was determined at each degree Celsius between 12 and 20°C after acclimation for at least two months in the culture cabinet (two to three cultures). Since no growth was observed at 12°C, cultures were acclimated at 13°C prior to the growth rate estimation at 12°C. Maximum growth rates at each temperature were estimated using a nonlinear regression procedure (NLREG software by P. H. Sherrod: Dennis *et al.* 1981).

(b) *Viability test*

Q2 Fluorescein diacetate (FDA) is non-fluorescent and apolar. It was added to cell suspensions to allow the viable cells to be counted. After entering the cell, it may be hydrolysed into fluorescein by non-specific esterases. If the cell membrane is intact, fluorescence which is polar accumulates in the cell. It is therefore a marker of esterases activity and membrane integrity, and therefore is an index of cell viability. FDA dissolved in acetone (1 mg ml^{-1}) is added to the cell suspension (2 μl ml^{-1}), which is incubated in the dark for 10 min. The proportion of viable cells (number of green cells per total number) is estimated under epifluorescence in at least 200 cells.

(c) *Synthesis of the all-*cis*-octadecapentaenoic acid*

The lability of the all-*cis*-octadecapentaenoic acid identified previously as one of the major agents toxic to *K. mikimotoi* (Parrish *et al.* 1993) prevents any direct estimation of the dose–effect relationship on phytoplankton cells. This fatty acid was synthesized in sufficient amounts (approx. 100 mg), according to the method described by Kuvlev *et al.* (1992), a method involving a γ-iodolactonization of 22 : 6n3. This method has previously been used to identify the mode of action of *K. mikimotoi* toxic principle (Fossat *et al.* 1999; Sola *et al.* 1999). The structure of the synthesized fatty acid was confirmed by GC–MS, FAB–MS, IR and ^{1}H-NMR and by comparison with a sample isolated from cultures. The standard fatty acid mixture contained 82% 18 : 5n3, the major impurities being 20 : 5n3 (5.4%), 18 : 4n3 (2%) and 22 : 6n3 (1%) fatty acids. The fatty acid was stored immediately after synthesis in vacuum-sealed ampoules in aliquots of approximately 100 mg at -20°C in the dark. The content of each ampoule was dissolved in 1 ml methanol and the exact fatty acid weight determined by weighing. Possible degradation of the fatty acid into aldehydes and oxidation products with a shorter retention time was checked by GC prior to any toxicity testing. Experiments were conducted with fatty acid standard above 90% purity.

(d) *Oxygen radical production measurements*

Degradation of the fatty acid was followed indirectly by trapping the oxygen radical trap HPPA (hydroxyphenylpropionic acid), of the hydroxyl radicals produced, following the method described by Palenik & Morel (1988). HPPA is oxidized into a fluorescent dimer measured by fluorescence (excitation 320 nm; emission 410 nm). Increase in fluorescence provides an integral measurement of the oxygen radicals produced. Estimation of the half-life of the fatty acid was measured in the dark at ambient temperature (18°C).

(e) *Toxicity of the all-*cis*-octadecapentaenoic acid*

The autotoxic effect of the 18 : 5n3 was tested in 50 ml aliquots of *K. mikimotoi* cultures. The fatty acid standard was dissolved in 1 ml methanol. The maximum volume added to test vials was 70 μl. Blanks were performed with 70 μl pure methanol in 50 ml cell suspensions. All measurements were done in triplicate. The concentration of viable cells was determined as described above.

(f) *Cell behaviour measured by laser sheet trajectography*

Cell behaviour was observed by laser sheet trajectography. An argon laser source was tuned at 488 nm, conditioned through a polarizer and a half-wavelength slide and through an optoacoustic deflector (AA-DTS-X-250). After the adjustment of the conditioning optics in order to maximize intensity of the first-order diffraction and minimum intensity for the zeroth order (18° incidence), a cylindrical lens was used to obtain a light sheet. An intensified NanoCam camera equipped with a 50 mm Nikon lens mounted back to front allowed a 22 enlargement factor. Sharp cell

images could be obtained with a shutter speed of 1 ms. The camera was mounted on a motorized stage allowing controlled displacements. Synchronization and generation of pulses for the optoelectronic deflector was performed by PASCAL software through an IEEE-488 bus, a multifunction and impulse generator. The motorized stage was driven through an RS-232. After calibration of the depth of the field, it was then possible to measure cell concentration and, by superposition of successive frames, to measure cell speed. In the descending plumes, cell concentration was so high that only movements of the fronts of the clouds of cells could be used to assess velocity measurements.

(g) *Migration experiments*

Aliquots of cultures at least 10 days old were transferred to square-sectioned cells (5×5×25 cm) at least 12 h prior to the experiment. Three millilitres of distilled water were added carefully at the water surface. Under light, the cells tended to concentrate in a surface layer from which descending plumes developed. An apparent steady state, as judged from the length of the descending plumes, developed in approximately 2–3 h. Before the establishment of descending plumes, underlying water was gently siphoned out. The elevated cell concentration remaining in the cell was counted every 30 min for 1.5 h. Each experiment was conducted in triplicate. After incubation periods, an FDA viability test was performed and each vial was counted for live cells after a 10 min incubation period in the dark.

(h) *One-dimensional physical modelling*

The hydrodynamic model is a one-dimensional dynamical and numerical model forced by wind and tide. In order to simulate tidal effects, free surface elevation gradients are considered. The model has five state variables, namely temperature, salinity, velocities (u, v) and turbulent kinetic energy. The turbulence closure is achieved by an algebraic formulation of the mixing length.

The two components of the velocity were

$$\begin{cases} \dfrac{\partial u}{\partial t} - fv = -g\dfrac{\partial \xi}{\partial x} + \dfrac{\partial}{\partial z}\left(n_z \dfrac{\partial u}{\partial z}\right) \\ \dfrac{\partial v}{\partial t} + fu = -g\dfrac{\partial \xi}{\partial y} + \dfrac{\partial}{\partial z}\left(n_z \dfrac{\partial v}{\partial z}\right) \end{cases}, \tag{2.1}$$

where t is the time; z is the vertical coordinate (positive upward); u is the E–W velocity (m s^{-1}); v is the N–S velocity (m s^{-1}); g is the gravitational acceleration (9.81 m s^{-2}); f is the Coriolis parameter (10^{-4} s^{-1}); n_z is the vertical eddy viscosity (m^2 s^{-1}); and $(\partial\xi/\partial x)$, $(\partial\xi/\partial y)$ is the free surface elevation gradient.

The surface condition was

$$n_z\left(\frac{\partial u}{\partial z}, \frac{\partial v}{\partial z}\right) = \left(\frac{\tau_x}{\rho}, \frac{\tau_y}{\rho}\right),$$

the surface wind stress components where ρ is the density of seawater (kg m^{-3}).

The bottom condition was

$$n_z\left(\frac{\partial u}{\partial z}, \frac{\partial v}{\partial z}\right) = C_d\sqrt{u_b^2 + v_b^2}(u_b, v_b),$$

where C_d is the drag coefficient (2.5×10^{-3}) and u_b, v_b are the velocities in the bottom layer.

For tidal forcing, we applied the linear theory of tide which indicates that the horizontal gradient induced by a tidal wave propagating in one direction can be expressed as the following horizontal gradient:

$$\left(\frac{\partial \xi}{\partial x}, \frac{\partial \xi}{\partial y}\right) = \frac{U_0}{gT}\left(\cos\left(\frac{2\pi t}{T}\right), \sin\left(\frac{2\pi t}{T}\right)\right),$$

where T is the M_2 tidal period (44 712 s) and U_0 is the maximum tidal current reached during a tidal cycle.

The turbulence closure model was based on the turbulence kinetic energy (TKE) state equation and an algebraic formulation of the mixing length (Luyten *et al.* 1996)

$$\frac{\partial k}{\partial t} = \frac{\partial}{\partial z}\left(n_z \frac{\partial k}{\partial z}\right) + P_s + G - \varepsilon,$$

Q3 where k is the turbulent kinetic energy (TKE: m^2 s^{-2}); ε is the dissipation rate of TKE (m^{-2} s^{-3}); production of TKE by vertical velocity gradient: $P_s = n_z((\partial u/\partial v)^2 + (\partial v/\partial z)^2)$; reduction of TKE by vertical density gradient: $G = -gk_z(1/\rho)(\partial\rho/\partial z)$; and k_z is the vertical eddy diffusivity (m^2 s^{-1}). In the chosen turbulence closure scheme, ε is given by a function of TKE and the mixing length l according to the following equation:

$$\varepsilon = \varepsilon_0 \frac{k^{\frac{1}{2}}}{l},$$

where $\varepsilon_0 = 0.166$ and $l_z = \kappa z(1 - z/H)^{1/2}$, with Karman constant $\kappa = 0.4$ and H is the depth of the water column.

Q4 Finally, turbulent eddy viscosity and eddy diffusivity are given by $n_z = S_u k^2/\varepsilon$, where S_u and S_b are the stability functions, the expressions of which can be found in Luyten *et al.* (1996).

Though similar to that of Westgard (1989), our model differs from it in two ways. In our model, (i) tidal current is taken into account (which was not the case in Westgard 1989) and (ii) ε is estimated as a function of the mixing length (we have a one-equation k closure scheme and not a two-equation k-ε closure scheme as in Westgard 1989). Luyten *et al.* (1996) compared different turbulence closure schemes for shelf stratified waters and concluded that there was no difference in the results between the two schemes, and the k closure scheme being less computer intensive. This model can be applied to situations with homogeneous or stratified vertical profiles of temperature and salinity; in particular, it can accommodate any type of gradient in turbulent eddy diffusivity due to complex haloclines on the shelf under the influence of river plumes. The model can also estimate the steady state vertical distribution as well as time-dependence distributions.

3. RESULTS AND DISCUSSION

We investigated the behaviour of *K. mikimotoi* in still cultures, and then applied the results in a simplified one-dimensional model in order to test the importance of crowding on population dynamics as a control process.

(a) *In vitro* cultures of *Karenia mikimotoi*

When cultured in batch, phytoplankton species follow a growth described by the logistic equation that takes into account an asymptotically stable census limit. In the case of our strain of *K. mikimotoi*, the maximum cell concentration reached in batch cultures never exceeded 4×10^{7} cell l^{-1}. Assuming a Poisson distribution (Rothschild 1992), the mean nearest neighbour distance at this cell concentration C is $d=0.55C^{-1/3}=$ 175 μm. Each cell requires on average a vital volume that corresponds to a travel time of roughly 2 s, as measured from laser sheet trajectography of individual cells. It should be noted that during these experiments in still cultures, cell collisions were never observed.

Different bioactive agents have been reported to be excreted by *K. mikimotoi*, namely the all-*cis*-3,6,9,12,15-octadecapentaenoic acid (in short 18 : 5n3) and its glycerides (Parrish *et al.* 1993), as well as three volatile sesquiterpenoids (Kajiwara *et al.* 1992). The volatile sesquiterpenoids appear to be rather stable in culture conditions, but unfortunately, their production has not been studied in detail. Parrish *et al.* (1994) showed that the concentrations of 18 : 5n3 vary greatly with environmental (temperature and light) culture conditions. It can reach 34% of total fatty acids at 18°C and 35 μE m^{-2} s^{-1}. This fatty acid inhibits Na-, K- and Mg-ATPase activities in a non-specific way (Fossat *et al.* 1999; Sola *et al.* 1999), and it could therefore act on different biological targets. Furthermore, these authors showed that toxicity from oxygen-free radicals produced by the degradation of the fatty acid was not involved in the process.

The lability of the octadecapentaenoic acid precluded the testing of extracts of *K. mikimotoi* culture medium on itself. The fatty acid was therefore synthesized from 22 : 6n3 using a γ-iodolactonization step, as described in §2. After checking the stereochemistry and purity, the LC_{50} for *K. mikimotoi* was found to be 1.5×10^{-4} M (figure 1). Controls consisting of 70 μl pure methanol gave results under 3% mortality. It clearly shows that *K. mikimotoi* is sensitive to its own toxin but to a lesser degree than potential competitors, as 1 μM 18 : 5n3 inhibits totally *Chaetoceros gracile* growth (Gentien 1998). These concentrations should not be extrapolated to nature as the fatty acid adsorbs on the wall, and on the air–water interface. In nature, the toxic agent is distributed around the producing cells and not dissolved in the aqueous phase; this renders the extrapolation even more difficult. However, this test demonstrates a different sensitivity of the two biological targets.

Allelopathic properties in *K. mikimotoi* have been demonstrated (Gentien & Arzul 1990; Arzul *et al.* 1993): they provide to this species a competitive advantage over the other phytoplankton species. However, the sensitivity of *K. mikimotoi* to its own toxin could counteract this advantage. In order to estimate the potential effect of this compound released at the cell membrane, it is essential to define how it is distributed around the cell.

To this effect, its half-life was measured indirectly by trapping the oxygen radicals produced by its degradation to HPPA. The increase in fluorescence due to the HPPA dimer formation gives an integrated measure of oxygen radicals produced during the decay

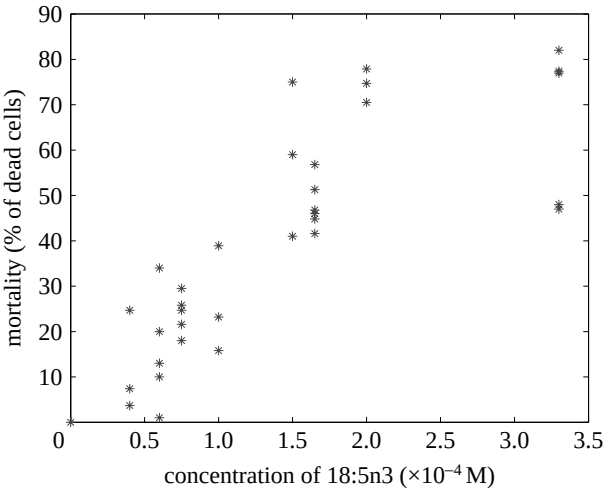

Figure 1. Dose–effect titration of the all-*cis*-3,6,9,12,15-octadecapentaenoic acid on *Karenia mikimotoi*.

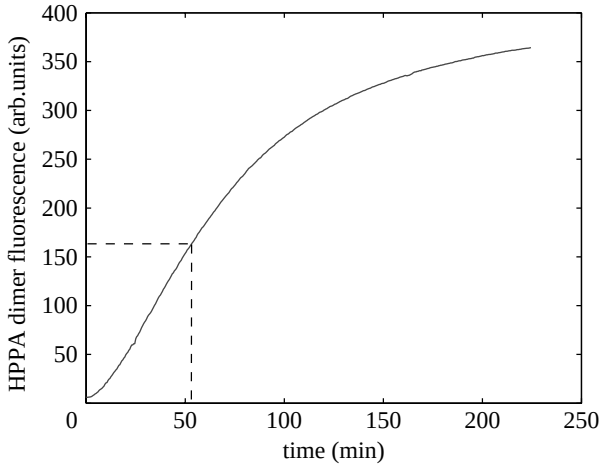

Figure 2. Integrated production of oxygen radicals during degradation of the 18 : 5n3 fatty acid (as estimated from the formation of the fluorescent dimer of hydroxyphenylpropionic acid).

of the 18 : 5n3 (figure 2). The half-life of this molecule in seawater and in the dark at 18°C is approximately 50 min. This half-life should be regarded as a maximum, since decay of degradation products can produce extra radicals. The average vital distance between cells could result from a balance between the flux from the cell and the molecular diffusion on the one hand and the toxin degradation and the LC_{50} on the other hand. Owing to the rapid decay of the toxin excreted by the cells, the action distance is very short and the estimated distance of 175 μm seems to be the upper limit. When transported in the viscous range, cells that continuously produce the toxin transport their own cloud of toxin.

Even if the time required for the toxin to act irreversibly is unknown, any increase in cell concentration would have a negative effect on cell viability. In culture, during the dark phase, cells tend to be evenly distributed throughout the culture volume, but during the light phase, cells crowd at the air–water interface in very thin layers (2–5 mm in thickness). Thus, cell concentration can locally be much higher than the average limit concentration in a culture. Subsampling in the surface layer showed local cell concentration over

3×10^8 cell l^{-1} (average neighbour distance of approx. 90 μm). The apparent contradiction with the observations reported above can be solved by a careful analysis of the processes. While the surface layer concentrates, descending plumes from the surface layer are observed. These descending plumes are so concentrated in cells that it was impossible to identify individual cells with the visualization system. Once the maximum vertical extent of the plume was reached, cells separated from their plume and progressively reached the surface layer at instantaneous speeds of 90–100 μm s^{-1} on average. This speed is similar to that observed for individual cells in the dark phase, but under illumination, the azimuths of the trajectories (data not shown) are oriented towards the surface resulting in a continuous cell exchange between surface layer and underlying water. This phenomenon, called 'bioconvection', has been described for many flagellates (Hopkins & Fauci 2002). As reported by Harashima *et al.* (1988), the essence of this phenomenon is that gravity acts on the concentrated layer, not on the water or micro-organisms separately but on their mixture. The energy source of bioconvection is the active transport of buoyancy given internally by the upward swimming of micro-organisms. These patterns increase the vertical diffusion of dissolved compounds released by cells, including possible exotoxins. Continuity requires an inflow of underlying water to compensate for the flux driven by descending plumes. If the residence time in the underlying water is sufficient, then the toxin would decay and the compensating flux to the surface layer would be free of toxin.

The speed of the descending plume front was observed to be approximately 200 μm s^{-1}. The upper part of the plumes can be approximated as cylinders of 4–6 mm (measured with the laser sheet system equipped with the optoelectronic deflector). These plumes induce a downward flux from the surface layer of 15.7 mm^3 s^{-1} per plume. Three to five plumes were observed in the 5×5 cm section containers. The total downward flux for an average of three plumes is in the range 30–68 mm^3 s^{-1}. The renewal time of water in the surface layer is between 1.2 and 7 min. Since no adverse effects on cell concentration were observed, this time is not sufficient at a distance of 90 μm to promote an irreversible effect on cells. The renewal time of underlying water is of the order of few hours, allowing the toxin to decay and the compensation water entering the surface layer to be free of toxin. This mechanism explains why cells do not suffer from crowding in the surface layer.

Q6 To confirm the hypothesis that a high residence time is necessary for the toxin to decay, underlying water was carefully withdrawn while the cell concentration was building up in the top layer. The results are illustrated in figure 3. The initial cell concentration in the concentrate is highly variable since it depends on various experimental conditions. The number of live cells was estimated (FDA measurements) after 180 min in the concentrate. On average, the final cell concentration observed in 12 experiments was 4×10^7 cell l^{-1}, with over 90% of the remaining cells still viable. This limit cell concentration is the one found in batch cultures.

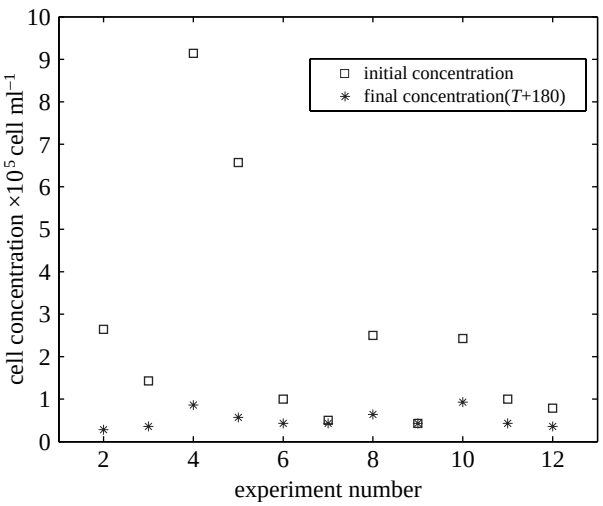

Figure 3. Evolution of cell concentration in 11 batches after withdrawal of the underlying dilution volume.

The importance of bioconvection in maintaining the crowded layer has been further confirmed by the following experiment. Bottom illumination of a culture flask blackened on the sides caused cell crowding at the bottom. Bioconvection could not occur in these conditions. After a light period of 4 h, all the cells had died; after return of the culture to normal illumination condition, the culture failed to grow again owing to the absence of a viable inoculum.

In summary, *K. mikimotoi* produces a short-lived toxin that acts at a short range. By the inhibition of competitors at low cell concentrations (10^4 cell l^{-1}), this toxin provides a competitive advantage (Arzul *et al.* 1993) but controls, at the same time, its own maximum cell yield. In quiet conditions, the phototropism-driven cell behaviour leads to local accumulation of cells without negative effects on cell concentration owing to the exploitation of physical instabilities.

The range of action of the toxin is the result of a balance between the production flux at the cell membrane, the molecular diffusion and the toxin decay rate. Local saturation of the medium does not occur since the toxin is unstable and the toxic effect acts only at a short distance. This finding is in accordance with the report by Uchida *et al.* (1999) that the inhibitory effect of *K. mikimotoi* on *Heterocapsa circularisquama* in bialgal cultures occurred mainly by direct cell contact. Therefore, allelopathic and autotoxic processes have an action at a short range (less than 175 μm). Hereafter, *K. mikimotoi* are considered as virtual particles with a maximum diameter of 175 μm.

We further examined the implications of this intrinsic property of *K. mikimotoi* on its own population development under realistic conditions.

(b) *In situ* population development

A common feature in field observations of *K. mikimotoi* is that it often occurs in or near the pycnocline layer during some stage of its population development. There are cases where populations develop in weakly stratified water bodies. However, along the Atlantic coast of Europe, blooms occur mainly on the stratified side of hydrographic fronts (Partensky & Sournia 1986). Blooms in stratified water columns remain

RSTB 20072079—2/4/2007—07:12—SRIKANTH—273602—XML RSB – pp. 1–11

confined mainly within the pycnocline layers (Birrien *et al.* 1991). Bjoernsen & Nielsen (1991) studied the distribution of *G. aureolum* in a pycnocline layer in the Kattegat with a high-resolution sampler. They observed a strong heterogeneity of the dinoflagellate population in the decimetre scale and concluded that *G. aureolum* formed at that time a more or less coherent 'magic carpet' in the pycnocline layer. These authors supposed that the inhibition of potential predators could be an important factor in the maintenance of a high phytoplankton biomass in the pycnocline layer.

Karenia mikimotoi has been shown to produce exotoxins that are detrimental to the growth of other algae (Gentien & Arzul 1990). On the Ushant front, *K. mikimotoi*'s maximum concentration corresponded to a minimum in diatoms (Arzul *et al.* 1993), and the minimum cell concentration for a reduction in the diatom growth rate was approximately 10^4 cell l^{-1} (Gentien 1998). Therefore, allelopathy exerted by *K. mikimotoi* may have been playing an effective role at the onset of the population development. We reported above that this adaptive advantage may be countered by autotoxicity above a limit in cell concentration; it could be that the population thus benefits from this confinement in a layer while, at the same time, being limited by this same confinement.

In §4, we test the hypothesis that the exotoxin production is an essential control factor in the population dynamics. Hereafter, we consider that two cells encounter when the vital volumes of these two cells intersect. Under quiet conditions *in vitro*, motile cells have the possibility to avoid each other. *In situ*, cells are transported and they may enter in 'contact' and turbulence would increase, at a given cell concentration, the frequency at which individual cells are within a certain distance of another. We treated this increase in frequency as the encounter of virtual particles with a diameter range between 25 μm (the cell diameter) and 175 μm (the vital volume around each cell).

Encounter rate is a function of sizes of colliding particles, their concentrations and environmental parameters. The encounter rate of particles is given by $\beta_c C^2$, where C is the concentration of particles and β_c is the coagulation kernel (product of the encounter kernel (β) and the efficiency kernel (α)). The encounter kernel represents the average percentage of particle pairs that will encounter per unit time and unit volume. It is the sum of the terms describing the different processes that bring particles into contact. Three major processes can generate encounter: Brownian motion; differential sedimentation; and shear (Pruppacher & Klett 1978, adapted by Jackson 1990).

Owing to their own motility, cells present a cell diffusivity that could be treated in the same way as Brownian motion if the cells were colliding in still conditions. Measurements of cell distance show that cells always maintain a minimum distance between them: collisions or cell doublets have never been observed, under quiet conditions. Even if the cell diffusivity is quite high, it can be supposed that in turbulent conditions, cell diffusivity does not have an important contribution to the encounter kernel.

Differential sedimentation means that each large settling particle generates a wake with a downward-induced motion. Such a large descending particle is expected to accumulate a cluster of smaller ones in its wake. The observations of cells in contact show a release of intracellular material due to lysis. In the first approximation, we suppose that released matter would be in the form of colloids, with a zero sedimentation speed. This process was therefore neglected.

The third encounter mechanism is due to shear: differences in fluid velocity cause two particles to approach each other. Considering only the latter mechanism and the fact that only the same-sized particles are concerned, the encounter kernel formulation for particles of the same size reduces to $\beta = \beta_{Sh} = 10.4\gamma r^3$ according to Pruppacher & Klett (1980), where γ is the shear rate (s^{-1}) and r (μm) is the cell active diameter which can be larger than the cell diameter. The term expressing mortality will therefore be formulated as follows: $-K\gamma C^2$, where γ is the shear rate (s^{-1}) ($\gamma = \sqrt{(\varepsilon/7.5v)}$), where ε is the energy dissipation rate and v is the kinematic viscosity (Moum & Lueck 1985); C is the cell concentration (m^{-3}); and K is a scaling parameter that takes into account the effective cross-section diameter and a scaling factor ($K = 0.1$ for cell concentration expressed in dm^{-3}).

The effect of the mortality process due to autotoxicity was tested under real conditions occurring on the Ushant front. The Iroise Sea, off West Brittany (France), in the eastern North Atlantic, shows a tidal and seasonal well-developed frontal system, the northern part of which was previously described as the Ushant front, well described for its physical, chemical and biological properties (Pingree *et al.* 1975, 1977). This area was selected as communities of dinoflagellates, including *K. mikimotoi* recur frequently in the pycnocline layers on the stratified side of this tidal front (Holligan & Harbour 1977). Realistic forcing has been applied to a one-dimensional model with realistic tides. Wind data have been obtained from the Ushant meteorological station.

Growth formulation was kept as simple as possible to test the effect of mortality induced by cell encounter. The maximum growth rate was observed to be 0.6 d^{-1} (Gentien 1998). The growth rate relation to temperature was obtained by a polynomial fit to *in vitro* measurements: $(\mu = 2.5\times10^{-3}T^3 - 0.15T^2 + 2.8775\,T - 17.25)$. This equation reproduces the zero growth rate observed at 12°C for this strain. The relative stability of maximum growth rate (more than 0.5 d^{-1}) between 14 and 18°C reflects probably the acclimation time allowed before growth rate measurements at different temperatures.

The pigment composition and bio-optical characteristics of *K. mikimotoi* being very plastic with respect to adaptation to the growth light regime allow it to benefit from both low and high levels of light (Johnsen & Sakshaug 1993). A light regime such as those reported from the pycnocline layers (1–5% incident light) during summer can support net growth of the population, albeit at non-saturated rates (Richardson & Kullenberg 1987). In the first approach, light limitation was not considered at all, even if this 1%

RSTB 20072079—2/4/2007—07:12—SRIKANTH—273602—XML RSB – pp. 1–11

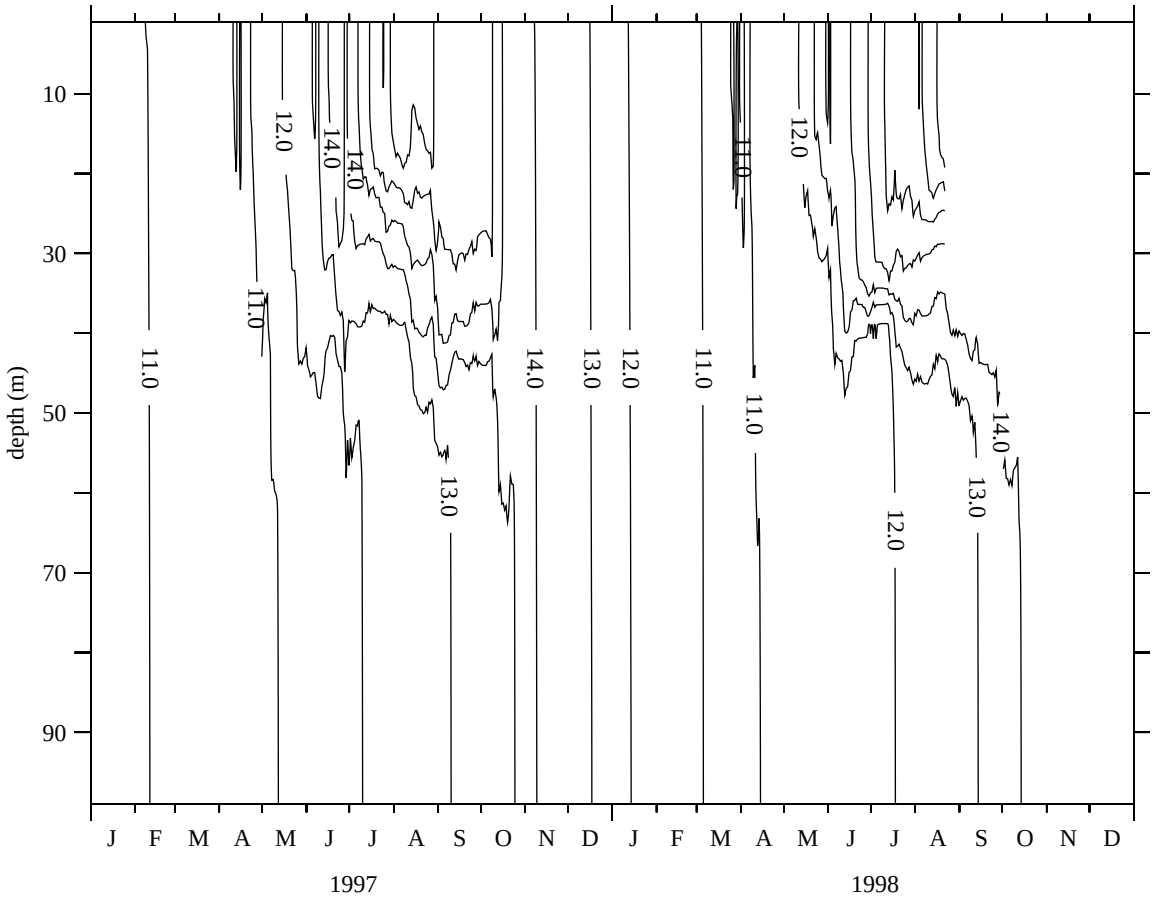

Figure 4. Modelling results using meteorological forcing time-series (1996–1998) from Ushant meteorological station: temperature evolution (Julian days starting from 1 January 1997).

limit may be encountered around 25–30 m depth in summer.

In stratified water columns, cells do not migrate and remain in the pycnocline layer. This has been considered as a fact and a model of vertical migration was not implemented. The explanation of this shift in behaviour should be the subject of further work.

The time evolution of the tracer *K. mikimotoi* is Q10 therefore

$$\frac{\partial C}{\partial t} = \frac{\partial}{\partial z}\left(k_z \frac{\partial C}{\partial Z}\right) + \mu(T)C - K\gamma C^2.$$

This model was run under realistic forcing for the years 1996–1998. K was kept constant at 5×10^{-5} (for a cell concentration expressed in cell l^{-1}), even if it is probable that K varies according to the cell physiological status. Mucopolysaccharides excretion would tend to lower γ at a given energy dissipation rate (ε) by local changes in the kinematic viscosity (ν). This process was not considered in this first approach model.

Initial conditions were set at the level of 1 cell l^{-1} distributed in the water column, with no reset during Q9 wintertime. figures 4–6 show results from the model run with 50 evenly distributed layers in the 50 m depth water column. It was started on 1 January 1996, but the stabilization period of the model is omitted from the figure and the results are presented for 1997–1998. Figure 4 represents the time–depth evolution of the isotherms: the gross features of the stratification offshore of the front are correctly reproduced in terms of temperature range and timing of the stratification. Figure 5 represents the evolution of the calculated shear rate resulting from the influence of wind events and the modulation of tidal friction on the bottom. Two low shear rate (less than 0.5 s^{-1}) periods occur at mid-depth in the summer months. During these periods, the *K. mikimotoi*-like tracer (figure 6) appears to develop in the pycnocline layer. The resulting pattern is similar to that reported by Holligan & Harbour (1977). The inset in figure 6 shows time discontinuities in cell densities closely associated with bursts of agitation induced by wind.

4. CONCLUSIONS

The ichthyotoxicity of *K. mikimotoi* is due to the production of a fatty acid (all-*cis*-octadecapentaenoic acid) or its glycoglycerolipids (Parrish *et al.* 1998). This fatty acid is labile, and therefore acts at local scales on algal competitors and other biological targets. Each cell of *K. mikimotoi* is surrounded by a cloud of toxin that does not exceed the 175 µm diameter. This toxin provides a competitive ecological advantage to *K. mikimotoi* over the other species encountered. However, *K. mikimotoi* cells are sensitive to their own toxins. Autotoxicity is a well-known process in terrestrial plants and has profound implications in agroecosystems (Singh *et al.* 1999). This is one of the few documented cases of autotoxicity in the marine environment (Pratt & Fong 1940; Imada *et al.* 1992). In culture, the possible autotoxicity in the case of cell crowding resulting from concentration of motile cells

RSTB 20072079—2/4/2007—07:12—SRIKANTH—273602—XML RSB – pp. 1–11

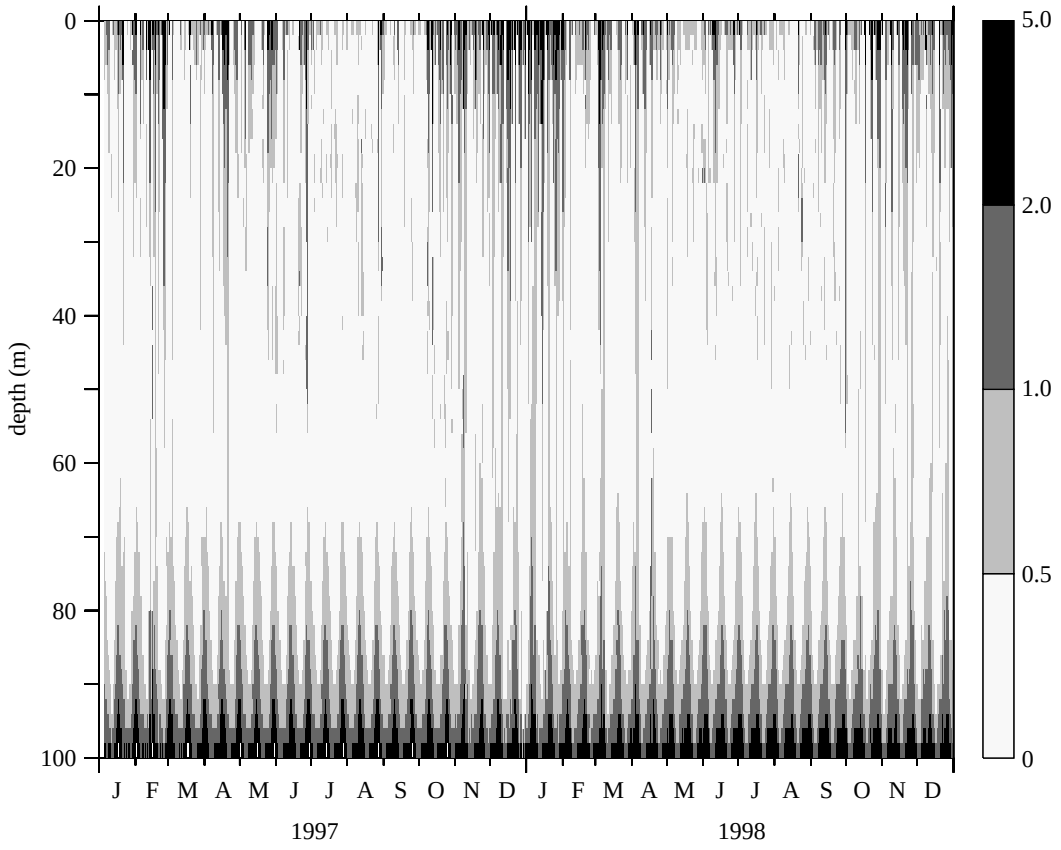

Figure 5. Modelling results using meteorological forcing time-series (1996–1998) from Ushant meteorological station: evolution of shear rate (s^{-1}).

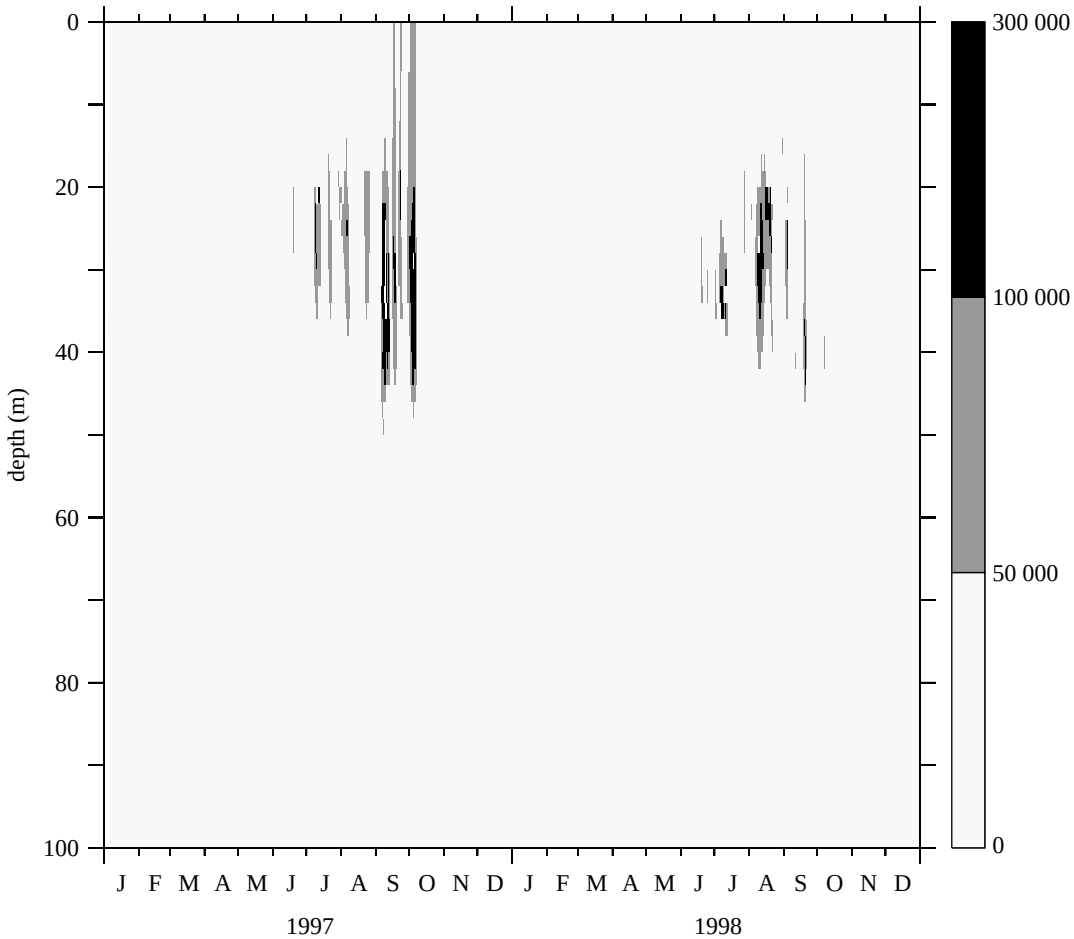

Figure 6. Modelling results using meteorological forcing time-series (1996–1998) from Ushant meteorological station: time and depth distribution of the *K. mikimotoi*-like tracer (isolines spacing: 5×10^4 cell l^{-1}).

RSTB 20072079—2/4/2007—07:12—SRIKANTH—273602—XML RSB – pp. 1–11

by phototropism was shown to be countered by the exploitation of physical instabilities.

The dependency on turbulence was tested as a major possible control in population dynamics. The modelling exercise should be considered as an experiment to evaluate the importance of this control process. To this effect, growth formulation has been kept as simple as possible, with a growth rate depending on temperature and mortality expressed by an encounter kernel depending solely on shear rate. This growth equation is similar in structure to the logistic equation used in still batch cultures with one major difference; that is, the mortality factor in C^2 depends on external forcing factors (tide and wind). Quite surprisingly, this simple formulation reproduces the gross features of the development of *K. mikimotoi* on the Ushant front. Population confinement in the pycnocline layer (Birrien *et al.* 1991; Gentien 1998) is not mainly driven by diurnal migration capabilities, as observed vertical distributions can be reproduced without using diurnal migration complex formulations. Hence, one can conclude that the confinement in the pycnocline layer is probably not due to an active behaviour but due to an increased survival rate.

This approach differs from the general 'ecological' models derived from models of phytoplanktonic biomass, in which it does not consider the competition for nutritive substrate as the determinant of the competition outcome between the various phytoplanktonic species, but rather relies on intrinsic properties of a given species.

Ranking of control factors allows reduction in the number of parameters needed from several tens to six, four of them (the coefficients of) being experimentally measurable, and therefore allows improvement of the robustness of the model. The higher the cell concentration, the higher will be the mortality rate. The population dependency on shear rate is likely to control the termination of the bloom more effectively than the possible depletion in nutrients. This result should be further investigated for these hydrodynamic conditions, using better shear rate estimates and a better understanding of the processes leading to collision between cells. This simple scheme may need some adaptation for shallow weakly stratified seas, where biological control factors may be more important than the physical ones. Nonetheless, the rate of cell mortality due to encounters should be considered as one of the major control factors of the population growth for this species.

5. UNCITED REFERENCE

Holligan (1978).

Q11

This work was supported by the IFREMER program ALTOX and partly by the EC-INTERREG programme NEMEDA. Fruitful discussions with Prof. T. Osborn and Dr I. R. Jenkinson are gratefully acknowledged.

REFERENCES

Arzul, G., Erard-Le Denn, E., Videau, C., Jegou, A. M. & Gentien, P. 1993 Diatom growth repressing factors during an offshore bloom of *Gyrodinium* cf. *aureolum*. In *Toxic phytoplankton blooms in the sea* (eds T. J. Smayda & Y. Shimizu), pp. 719–724. Amsterdam, The Netherlands: Elsevier Science Publishers.

Berdalet, E. 1992 Effects of turbulence on the marine dinoflagellate *Gymnodinium nelsonii*. *J. Phycol.* **28**, 267–272. (doi:10.1111/j.0022-3646.1992.00267.x)

Birrien, J. L., Wafar, M. V., Le Corre, P. & Riso, R. 1991 Nutrients and primary production in a shallow stratified ecosystem in the Iroise Sea. *J. Plankton Res.* **13**, 721–742. (doi:10.1093/plankt/13.4.721)

Bjoernsen, P. K. & Nielsen, T. G. 1991 Decimeter scale heterogeneity in the plankton during a pycnocline bloom of *Gyrodinium aureolum*. *Mar. Ecol. Prog. Ser.* **73**, 263–267.

Dennis, J. E., Gay, D. M. & Welsch, R. E. 1981 An adaptive non-linear least-squares algorithm. *ACM Trans. Math. Software* **7**, 348–369. (doi:10.1145/355958.355965)

Erard-Le Denn, E., Morlaix, M. & Dao, J. C. 1990 Effects of *Gyrodinium* cf. *aureolum* on *Pecten* maximus (post larvae, juveniles and adults). In *Toxic marine phytoplankton* (eds E. Granéli, B. Sundström, L. Edler & D. M. Anderson), pp. 132–136. Amsterdam, The Netherlands: Elsevier Science Publishing Co., Inc.

Fossat, B., Porthe-Nibelle, J., Sola, P., Masoni, A., Gentien, P. & Bodennec, G. 1999 Toxicity of fatty acid 18 : 5n3 from *Gymnodinium* cf. *mikimotoi*: II. Intracellular pH and KC uptake in isolated trout hepatocytes. *J. Appl. Toxicol.* **19**, 275–278. (doi:10.1002/(SICI)1099-1263(199907/08)19:4<275::AID-JAT578>3.0.CO;2-B)

Gentien, P. 1998 Bloom dynamics and ecophysiology of the *Gymnodinium mikimotoi* species complex. In *Physiological ecology of harmful algal blooms*, vol. G41 (eds D. M. Anderson, A. D. Cembella & G. M. Hallegraeff). NATO ASI Series, pp. 155–173. Berlin, Germany: Springer.

Gentien, P. & Arzul, G. 1990 Exotoxin production by *Gyrodinium* cf. *aureolum* (Dinophyceae). *J. Mar. Biol. Assoc. UK* **70**, 571–581.

Franks, P. J. S. 1995 Thin layers of phytoplankton: a model of formation by near-inertial waves shear. *Deep-Sea Res. I* **42**, 75–91.

Harashima, A., Watanabe, M. & Fujishiro, I. 1988 Evolution of bioconvection patterns in a culture of motile flagellates. *Phys. Fluids* **31**, 764–775. (doi:10.1063/1.866812)

Holligan, P. M. 1978 Patchiness in subsurface phytoplankton populations on the Northwest European continental shelf. In *Spatial pattern in plankton communities NATO conference series*, vol. 3, pp. 221–238. New york, NY: Plenum Press. Pt. 4

Holligan, P. M. & Harbour, D. S. 1977 The vertical distribution and succession of phytoplankton in the western English Channel in 1975 and 1976. *J. Mar. Biol. Assoc. UK* **57**, 1075–1093.

Hopkins, M. M. & Fauci, L. J. 2002 A computational model of the collective fluid dynamics of motile micro-organisms. *J. Fluid Mech.* **455**, 149–174. (doi:10.1017/S0022112001007339)

Iizuka, S., Sugiyama, H. & Hirayama, K. 1989 Population growth of *Gymnodinium nagasakiense* red tide in Omura Bay. In *Red tides: biology, environmental science and toxicology* (eds T. Okaichi, D. M. Anderson & T. Nemoto), pp. 269–272. New York, NY: Elsevier.

Imada, N., Kobayashi, K., Isomura, K., Saito, H., Kimura, S., Tahara, K. & Oshima, Y. 1992 Isolation and identification of an autoinhibitor produced by *Skeletonema costatum*. *Nippon Suisan Gakkaishi* **58**, 1687–1692.

Jackson, G. A. 1990 A model of the formation of marine algal flocs by physical coagulation processes. *Deep-Sea Res.* **37**, 1197–1211. (doi:10.1016/0198-0149(90)90038-W)

Johnsen, G. & Sakshaug, E. 1993 Bio-optical characteristics and photoadaptive responses in the toxic and bloom-forming dinoflagellates *Gymnodinium aureolum*, *Gymnodinium galatheanum* and two strains of *Prorocentrum*

minimum. *J. Phycol.* **29**, 627–642. (doi:10.1111/j.0022-3646.1993.00627.x)

Juhl, A. R. & Latz, M. I. 2002 Mechanisms of fluid shear-induced inhibition of population growth in a red-tide dinoflagellate. *J. Phycol.* **38**, 683–694. (doi:10.1046/j.1529-8817.2002.00165.x)

Kajiwara, T., Ochi, S., Kodama, K., Matsui, K., Hatakana, A., Fujimura, T. & Ikeda, T. 1992 Cell-destroying sesquiterpenoids from red tide of *Gymnodinium nagasakiense*. *Phytochemistry* **31**, 783–785.

Koizumi, Y., Uchida, T. & Honjo, T. 1996 Diurnal vertical migration of *Gymnodinium mikimotoi* during a red tide in Hoketsu Bay, Japan. *J. Plankton Res.* **18**, 289–294. (doi:10.1093/plankt/18.2.289)

Kuvlev, D. V., Aizdaicher, N. A., Imbs, A. B., Bezuglov, V. V. & Latishev, N. A. 1992 All-*cis*-3,6,9,12,15-octadecapentaenoic acid from the unicellular alga *Gymnodinium kowalevskii*. *Phytochemistry* **31**, 2401–2403. (doi:10.1016/0031-9422(92)83286-8)

Le Corre, P., L'Helguen, S. & Wafar, M. 1993 Nitrogen source for uptake by *Gyrodinium* cf. *aureolum* in a tidal front. *Limnol. Oceanogr.* **38**, 446–451.

Luyten, P., Deleersnijder, E., Ozer, J. & Ruddick, K. 1996 Presentation of a family of turbulence closure models for stratified shallow water flows and preliminary application to the Rhine outflow region. *Cont. Shelf Res.* **16**, 101–130. (doi:10.1016/0278-4343(95)93591-V)

Moum, J. N. & Lueck, R. G. 1985 Causes and implications of noise in oceanic dissipation measurements. *Deep-Sea Res.* **32**, 379–392. (doi:10.1016/0198-0149(85)90086-X)

Palenik, B. & Morel, F. M. M. 1988 Dark production of H sub(2)O sub(2) in the Sargasso Sea. *Limnol. Oceanogr.* **33**, 1606–1611.

Parrish, C. C., Bodennec, G., Sebedio, J.-L. & Gentien, P. 1993 Intra- and extra cellular lipids in cultures of the toxic dinoflagellate, *Gyrodinium aureolum*. *Phytochemistry* **32**, 291–295. (doi:10.1016/S0031-9422(00)94983-5)

Parrish, C. C., Bodennec, G. & Gentien, P. 1994 Time courses of intracellular and extracellular lipid classes in batch cultures of the toxic dinoflagellate, *Gymnodinium* cf. *nagasakiense*. *Mar. Chem.* **48**, 71–82. (doi:10.1016/0304-4203(94)90063-9)

Parrish, C. C., Bodennec, G. & Gentien, P. 1998 Haemolytic glycoglycerolipids from *Gymnodinium* species. *Phytochemistry* **47**, 783–787. (doi:10.1016/S0031-9422(97)00661-4)

Partensky, F. & Sournia, A. 1986 Le dinoflagellé *Gyrodinium* cf. *aureolum* dans le plankton de l'Atlantique Nord: identification, écologie, toxicité. *Crypt. Algol.* **7**, 251–275.

Pingree, R. D., Pugh, P. R., Holligan, P. M. & Forster, G. R. 1975 Summer phytoplankton blooms and red tides along tidal fronts in the approaches to the English Channel. *Nature* **258**, 672–677. (doi:10.1038/258672a0)

Pingree, R. D., Holligan, P. M. & Head, R. N. 1977 Survival of dinoflagellate blooms in the western English channel. *Nature* **265**, 266–269. (doi:10.1038/265266a0)

Pollingher, U. & Zemel, E. 1981 *In-situ* and experimental evidence of the influence of turbulence on cell division processes of *Peridinium cinctum* forma Westii (Lemm.) Lefevre. *Br. Phycol. J.* **16**, 281–287.

Pratt, R. & Fong, J. 1940 Studies on *Chlorella vulgaris*: II. Further evidence that *Chlorella* cells form a growth-inhibiting substance. *Am. J. Bot.* **27**, 431–436. (doi:10.2307/2436459)

Pruppacher, H. R. & Klett, J. D. 1978 *The microphysics of clouds and precipitation*. Boston, MA: Reidel pp. 714

Richardson, K. & Kullenberg, G. 1987 Physical and biological interactions leading to plankton blooms: a review of a bloom of *Gyrodinium aureolum* blooms in Scandinavian waters. *Rapp. P.-V. Reun. Cons. Int. Explor. Mer.* **187**, 19–26.

Rothschild, B. J. 1992 Application of stochastic geometry to problems in plankton ecology. *Phil. Trans. R. Soc. B* **336**, 225–237. (doi:10.1098/rstb.1992.0058)

Singh, H. P., Batish, D. R. & Kohli, R. K. 1999 Autotoxicity: concept, organisms, and ecological significance. *Crit. Rev. Plant Sci.* **18**, 757–772. (doi:10.1080/07352689991309478)

Sola, P., Masoni, A., Fossat, B., Porthe-Nibelle, J., Gentien, P. & Bodennec, G. 1999 Toxicity of fatty acid 18 : 5n3 from *Gymnodinium* cf. *mikimotoi*: I. Morphological and biochemical aspects on *Dicentrarchus labrax* gills and intestine. *J. Appl. Toxicol.* **19**, 279–284. (doi:10.1002/(SICI)1099-1263(199907/08)19:4<279::AID-JAT579>3.0.CO;2-X)

Sullivan, J. M., Swift, E., Donaghay, P. L. & Rines, J. E. B. 2003 Small-scale turbulence affects the division rate and morphology of two red-tide dinoflagellates. *Harmful Algae* **2**, 183–199. (doi:10.1016/S1568-9883(03)00039-8)

Uchida, T., Toda, S., Matsuyama, Y., Yamaguchi, M., Kotani, Y. & Honjo, T. 1999 Interactions between the red tide dinoflagellates *Heterocapsa circularisquama* and *Gymnodinium mikimotoi* in laboratory cultures. *J. Exp. Mar. Biol. Ecol.* **241**, 285–299. (doi:10.1016/S0022-0981(99)00088-X)

Westgard, T. 1989 Two models for the vertical distribution of pelagic fish eggs in the turbulent upper layer of the ocean. *Rapp. P.-V. Réun. Const. Int. Explor. Mer.* **191**, 195–200.

Yamamoto, T. & Seike, T. 2003 Modelling the population dynamics of the toxic dinoflagellate *Alexandrium tamarense* in Hiroshima Bay Japan. II. Sensitivity to physical and biological parameters. *J. Plankton Res.* **25**, 63–81. (doi:10.1093/plankt/25.1.63)

Author Queries

JOB NUMBER: 20072079

JOURNAL: RSTB

Q1 Please check the inserted short title.

Q2 Please note the edit of sentences 'Fluorescein diacetate (FDA) was added to cell suspensions to allow…FDA is non-fluorescent and apolar'.

Q3 Please confirm if 'TKE' refers to 'turbulent kinetic energy' or 'turbulence kinetic energy'.

Q4 Please check the inserted variable 'Sb' in the sentence Finally, turbulent eddy viscosity and eddy diffusivity are given by…

Q5 Please check and approve the edit of the sentence '…the distance of 175 μm, estimated above, may be seen as an upper limit' to '…the estimated distance of 175 μm seems to be the upper limit'.

Q6 Please note that in section 3a, the paragraph 'To confirm the hypothesis that a high residence time is necessary for the toxin to decay…' given in bold has been changed to the normal font.

Q7 Reference Pruppacher & Klett (1980) has been cited in text but not provided in the list. Please supply reference details or delete the reference citation from the text.

Q8 Please note the edit of the term 'pycnocline levels' to 'pycnocline layers' in the sentence 'A light regime such as those reported from…'

Q9 Please note that figure citations 'figure 4a–c' have been changed to 'figures 4–6', respectively.

Q10 Please note that the word 'inset' has been mentioned in the sentence 'The inset in figure 6 shows time discontinuities…', but the same is not found in the figure. Please check.

Q11 Reference Holligan (1978) is provided in the list but not cited in the text. Please supply citation details or delete the reference from the reference list.

RSTB 20072079—2/4/2007—07:13—SRIKANTH—273602—XML RSB – pp. 1–11